ANNUAL REVIEWS

Annual Review of Condensed Matter Physics

Enzymes as Active Matter

Subhadip Ghosh,[1] Ambika Somasundar,[2] and Ayusman Sen[1,2]

[1]Department of Chemistry, The Pennsylvania State University, University Park, Pennsylvania 16802, USA; email: subhadip.chem@gmail.com, asen@psu.edu

[2]Department of Chemical Engineering, The Pennsylvania State University, University Park, Pennsylvania 16802, USA; email: ambika92@gmail.com

Annu. Rev. Condens. Matter Phys. 2021. 12:177–200

First published as a Review in Advance on November 23, 2020

The *Annual Review of Condensed Matter Physics* is online at conmatphys.annualreviews.org

https://doi.org/10.1146/annurev-conmatphys-061020-053036

Keywords

enzyme catalysis, self-propulsion, enhanced diffusion, chemotaxis, enzyme pumps, collective behavior

Abstract

Nature has designed multifaceted cellular structures to support life. Cells contain a vast array of enzymes that collectively perform essential tasks by harnessing energy from chemical reactions. Despite the complexity, intra- and intercellular motility at low Reynolds numbers remain the epicenter of life. In the past decade, detailed investigations on enzymes that are freely dispersed in solution have revealed concentration-dependent enhanced diffusion and chemotactic behavior during catalysis. Theoretical calculations and simulations have determined the magnitude of the impulsive force per turnover; however, an unequivocal consensus regarding the mechanism of enhanced diffusion has not been reached. Furthermore, this mechanical force can be transferred from the active enzymes to inert particles or surrounding fluid, thereby providing a platform for the design of biomimetic systems. Understanding the factors governing enzyme motion would help us to understand organization principles for dissipative self-assembly and the fabrication of molecular machines. The purpose of this article is to review the different classes of enzyme motility and discuss the possible mechanisms as gleaned from experimental observations and theoretical modeling. Finally, we focus on the relevance of enzyme motion in biology and its role in future applications.

1. INTRODUCTION

Enzymatic propulsion (1–6) is an excellent example of active dynamics (7–10), obeying low Reynolds number mechanics (11). In living systems, enzymes are responsible for promoting various metabolic activities. The catalysis by enzymes involves conversion of reactants (often termed as substrate) into products accompanied by release of energy. The energy output is used to perform essential tasks and sustain different physiological processes. As an example, eukaryotic cells have a complex network of motor proteins such as myosins, kinesins, and dyneins that possess the ability to perform random walk along predefined paths (12–15). These enzymes catalyze the hydrolysis of energy-rich adenosine triphosphate (ATP) molecules to release energy that translates into force fluctuations and/or mechanical work and initiates the active dynamics inside the cell (16–18). Experiments and modeling commonly estimate the force fluctuations to be ∼10 pN/catalytic turnover, which is utilized by the motor proteins in sensing load and transportation of cargo molecules (19). In contrast to motor proteins, freely dispersed enzymes in solution were previously thought to undergo passive diffusion without any actuation. However, it has recently been discovered that these enzymes, including those that promote non-ATP-driven reactions, display enhanced diffusive motion under out-of-equilibrium conditions (**Figure 1*a***) (12). Furthermore, the mechanical force generated in such enzymatic reactions is adequate to induce enzyme propulsion in a directed manner in response to chemical gradients, which is an example of molecular chemotaxis (1). The self-propulsive behavior of most enzymes was found to show substrate concentration dependence following the Michaelis–Menten kinetic model, further emphasizing the importance of catalysis in enzyme actuation (6, 20). Reaction-induced diffusiophoresis, conformational changes, or local environment changes near the catalytic site are likely factors for enhanced diffusion of enzymes in uniform substrate concentrations (6, 20–22). The driving force for gradient-based directed propulsion is attributed to the lowering of chemical potential due to favorable enzyme-substrate interactions (22).

The force fluctuations from active enzymes can be transferred to the surrounding environment (12). Anchoring enzymes on surfaces of particles or attaching them to a solid support results in self-powered vehicles or fluid pumps, respectively, with many potential applications (2, 25–28). In an origin-of-life scenario, enzymes that are part of a network can sense and communicate through signaling mechanisms and self-organize in response to external stimuli (29, 30). Similarly, active enzymes are believed to regulate the stochastic motion of the circulating fluids, form metabolons, and transport biological species to target locations throughout the physiological system (6). In this review, we focus on the physical chemistry of enzymatic motion at the molecular level based on enhanced diffusion, chemotaxis, and pumping. We also speculate on the significance of enzymatic forces in biology and their roles in cellular organization, transport, and physiological functions.

Active dynamics: processes pervading living systems and synthetic active matter that depend on a sustained supply of free energy, which they consume to produce work

Substrate: the chemical species or reactant that undergoes an enzyme-catalyzed chemical reaction to form products

Michaelis–Menten kinetic model: relates the enzyme-catalyzed reaction rate to reactant (substrate) concentration

Conformational changes: dynamic changes in the shape of a biomolecule

Metabolon: transient assemblies of enzymes participating in reaction cascades where the product from one enzymatic reaction is the substrate for the next

2. ENHANCED DIFFUSION OF ACTIVE ENZYMES

2.1. Experimental Observations of Enhanced Diffusion

The concept of powered enzyme diffusion is related to Purcell's model for motion at low Reynolds number and subsequent discovery of random walk by motor proteins inside the cell, utilizing energy from ATP hydrolysis (11, 13). In 2009, Muddana et al. first reported that the diffusion of freely dispersed urease molecules in buffer solution increases when the substrate urea is added to the medium (23). The enhancement in the diffusion coefficient of a single urease molecule occurred as a function of urea concentration that reached saturation only at high concentration of the substrate following the Michaelis–Menten kinetics (**Figure 1*b***). Inactivation of urease with pyrocatechol, however, resulted in attenuation of the diffusion coefficient. Subsequent publications

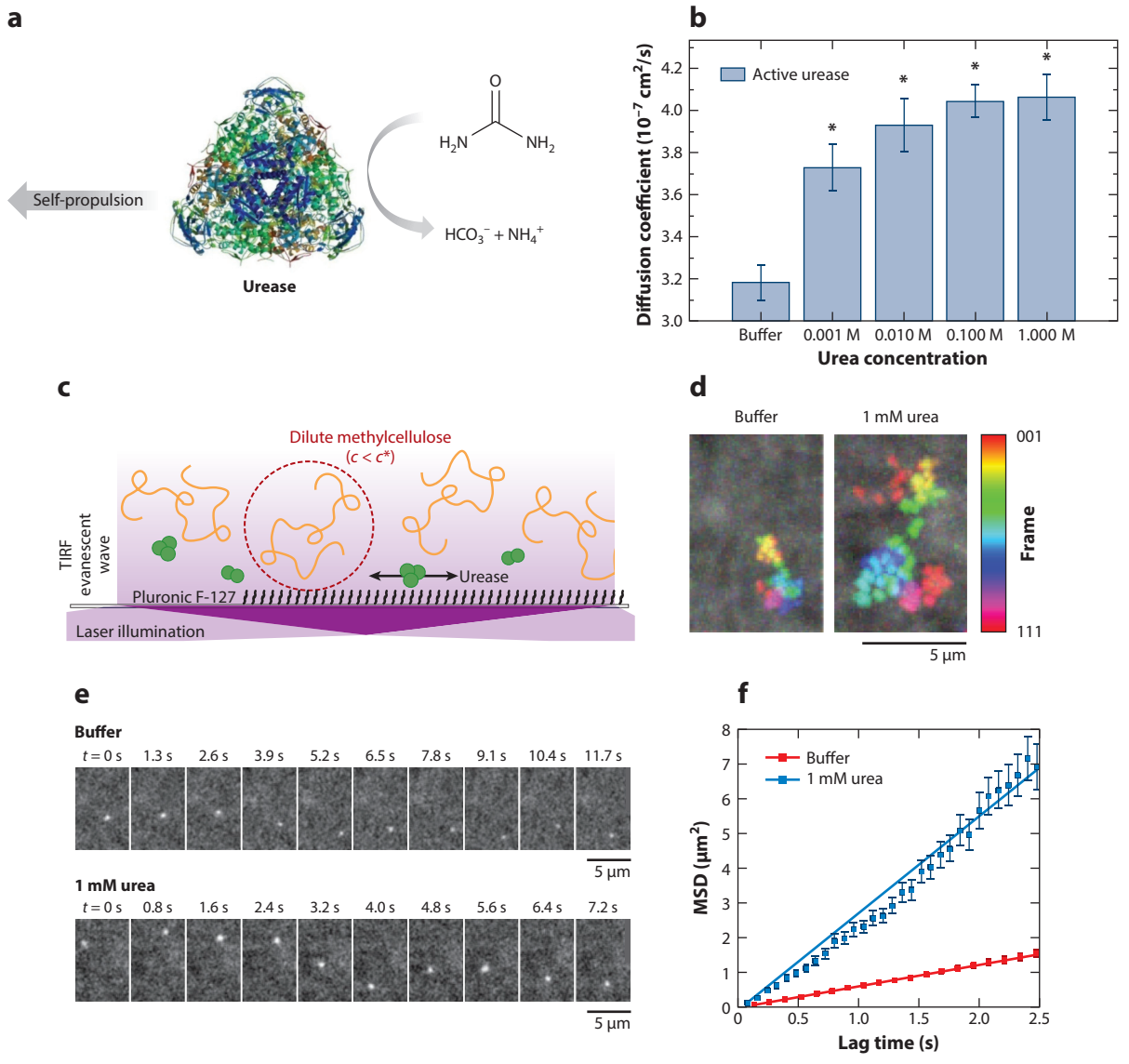

Figure 1

(*a*) Schematic representation showing the catalytic conversion of urea by urease, leading to self-propulsion. (*b*) Fluorescence correlation spectroscopy plot showing the changes in the diffusion coefficient of urease with increasing concentration of substrate urea. Asterisk (*) indicates a significance value of $p < 0.05$. (*c*) Experimental setup for single-particle imaging of urease using TIRF microscopy. (*d*) 2D trajectories of urease displayed as time-collapsed images, with color scale, representing the diffusion time over 111 frames, in buffer and in the presence of 1 mM of urea as marked in the image. (*e*) Time series of single urease molecules diffusing over time in buffer and in the presence of 1 mM of urea as marked in the image. (*f*) MSD versus time plot of each trajectory. Panels *a* and *b* adapted with permission from Reference 23; copyright 2010 American Chemical Society. Panels *c–f* adapted with permission from Reference 24; copyright 2019 American Physical Society. Abbreviations: MSD, mean squared displacement; TIRF, total internal reflection fluorescence.

Cofactor: a chemical species that promotes enzyme catalysis

by the Sen group demonstrated similar enhancement in diffusion for other enzymes like catalase and DNA polymerase in the presence of their substrate hydrogen peroxide (H_2O_2) and ATP, respectively, or a cofactor like Mg^{2+} (1, 31). Thus, catalysis was hypothesized to be the driving force for the diffusion changes. The diffusion measurements were carried out using fluorescence correlation spectroscopy (FCS) by labeling the enzymes with suitable fluorescent dyes and at low concentrations of the enzyme to ensure the presence of a single molecule in the observation volume. These experiments revealed that the diffusion was 30–50% higher at saturating substrate concentration compared to enzymes in only buffer or control medium (1, 23, 31). The enzyme aldolase that catalyzes an endothermic chemical reaction exhibited enhanced diffusion by FCS in the presence of the substrate fructose-1,6- bisphosphate (FBP) and also in the presence of the competitive inhibitor pyrophosphate (32). Zhao et al. took advantage of the stochastic fluctuation of diffusing enzymes to show that momentum is transferred during the catalytic activity of enzymes in solution to induce enhanced motion of passive particles (33). The results were further generalized by showing that the increase in diffusive motion of particles scales with the Stokes–Einstein equation. Enhanced diffusive motion was also measured by FCS for several enzymes associated with the glycolysis cascade involving hexokinase, phosphoglucose isomerase, phosphofructokinase, and aldolase. When the combination of enzymes was fed into a microfluidic channel through different inlets and a gradient of D-glucose, ATP, and Mg^{2+} (substrates and cofactor for hexokinase) was applied, the enzymes in the cascade exhibited gradient-based cross-diffusion in a sequential manner. This sequential directed migration or chemotaxis was proportional to the concentration of the respective substrates formed in the cascade (29). Sun et al. developed a facile route for real-time monitoring of enhanced diffusion within an enzyme cascade reaction. The enzymes were initially anchored to a DNA strand or an origami structure and subsequently incorporated in a lipid bilayer through cholesterol functionalities. The interplay of mobile and immobile DNA architectures allows the enhanced diffusion of the enzymes to be tracked precisely (34).

2.2. Recent Developments on the Diffusion of Active Enzymes

Consistent with the recent work on enhanced diffusion of enzymes, more than two decades ago Börsch and coworkers demonstrated that F_1-ATPase enzyme undergoes increase in diffusion in the presence of ATP owing to conformational changes (35). However, in a recent article, they claimed that the diffusion enhancement observed for F_1-ATPase was due to structural dissociation of the enzyme subunit upon substrate binding, which eventually moves faster than the larger, native enzyme. Furthermore, the reliability of the FCS technique that was used for diffusion measurements was questioned (36). Inspired by suggestions from Bai & Wolynes (37), Günther et al. (36) also carried out fluorescence lifetime experiments to show that enhanced diffusion reported for alkaline phosphatase enzyme with substrate p-nitrophenyl phosphate is most probably an artifact due to the quenching of the fluorescent dye (used for labeling the enzyme) in the presence of the photoactive product p-nitrophenol (38). These observations have led to further scrutiny of enzyme diffusion measurements by the FCS technique (39). In a recent article, Ghosh et al. explored the diffusive fluctuations due to the transmembrane enzyme Na^+/K^+ ATPase (commonly known as Na^+/K^+ pump) by reconstituting the enzyme in model phospholipid vesicle membrane and eliminating the possibility of enzyme subunit dissociation during experimental recordings (**Figure 2*a*,*b***) (40). Enhanced diffusion of the ATPase-tagged vesicle was not only observed with the conventional substrate ATP but also with other triphosphate substrates with the observed enhancement related to their specific catalytic turnover rates (42). Attaching two other enzymes, acid phosphatase and urease, on vesicle surface via biotin–streptavidin linkage also led to diffusion enhancement upon catalysis. Additional experiments were also conducted to rule out contributions from fluorescence quenching. Real-time optical microscopy coupled with mean

squared displacement (MSD) analysis supported the motile behavior of the enzyme-attached vesicles in the presence of substrate.

2.3. Enhanced Diffusion Observed from Different Experimental Techniques

To overcome the limitations of FCS, researchers explored alternative instrumental methods to study freely dispersed enzymes in bulk solution. Jee et al. resorted to high-resolution-based

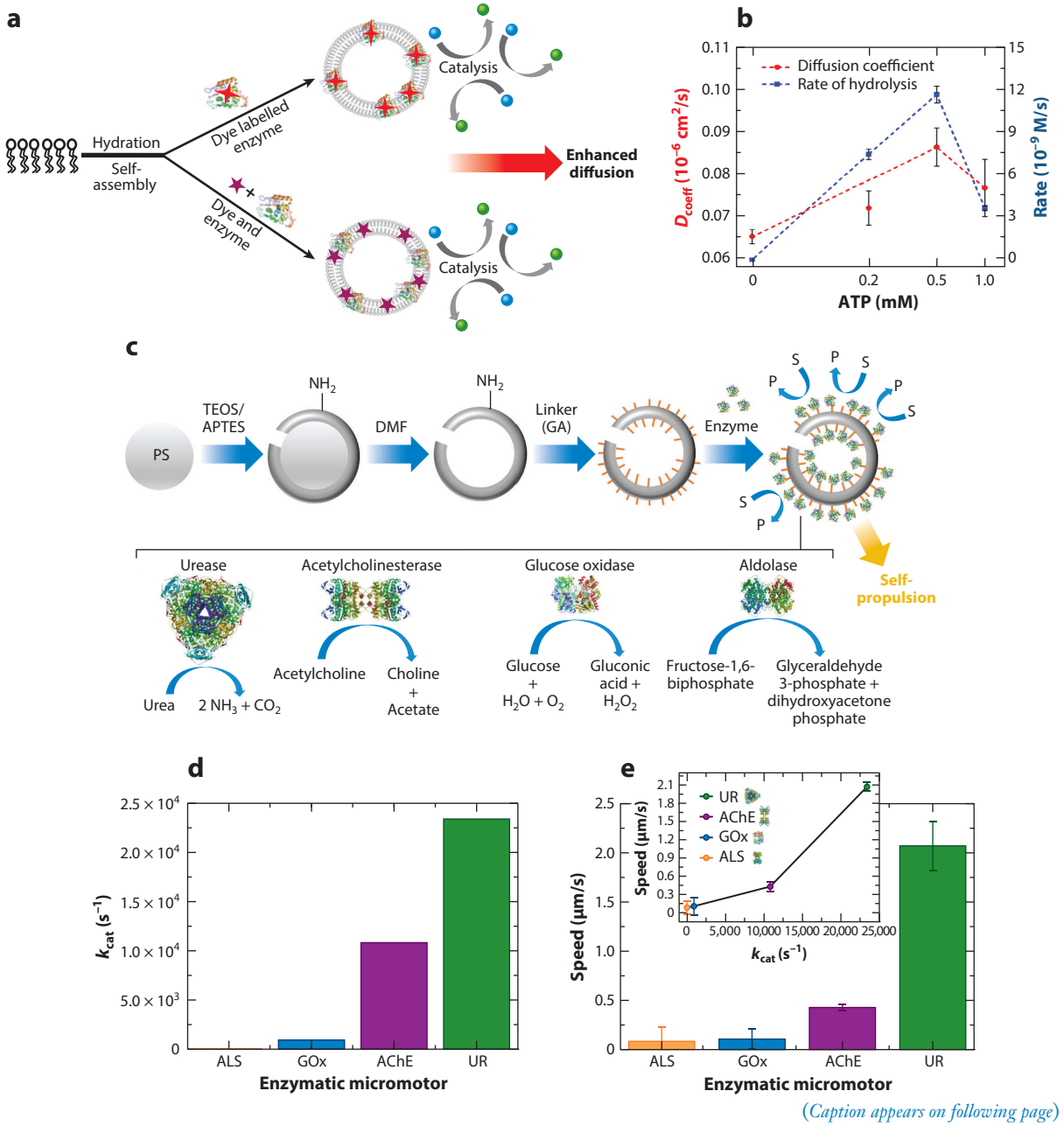

(Caption appears on following page)

Figure 2 (*Figure appears on preceding page*)

(*a*) Schematic representation showing the enhanced diffusion of an ATPase-tagged vesicle due to substrate turnover. (*b*) Overlay plot showing the rate of ATP hydrolysis with ATPase-tagged vesicles (*blue*) versus the diffusion data from fluorescence correlation spectroscopy (*red*) against ATP concentrations along the *x* axis. (*c*) Schematic representation showing the fabrication of HSMM functionalized with different enzymes that undergo catalytic reaction, resulting in self-propulsion. (*d*) Plot showing k_{cat} values from the literature for the different enzymes on HSMM. (*e*) Plot showing the average speeds of the different enzyme-attached HSMM for substrate concentrations that produce maximum self-propulsion. Inset shows the correlation between the speed of the HSMM and the k_{cat} of each enzyme. Panels *a* and *b* adapted with permission from Reference 40; copyright 2019 American Chemical Society. Panels *c–e* adapted with permission from Reference 41; copyright 2019 Springer Nature. Abbreviations: AChE, acetylcholine esterase; ALS, aldolase; APTES, 3-aminopropyltriethoxysilane; ATP, adenosine triphosphate; DMF, dimethylformamide; GA, glutaraldehyde; GOx, glucose oxidase; HSMM, hollow silica micromotors; P, product; PS, polystyrene; S, substrate; TEOS, tetraethyl orthosilicate; UR, urease.

stimulated emission–depletion fluorescence correlation spectroscopy (STED-FCS) to reproduce the enhanced diffusion of urease under catalytic conditions (43). The experimental setup of STED-FCS ensured diffusion measurements were resolved to subdiffraction spots in which single enzymes showing ballistic leaps can be captured with high precision. Acetylcholine esterase enzyme, which was also studied, displayed similar leaping behavior. In a different fluorescence-based setup, namely total internal reflection fluorescence microscopy, the Ross and Sen groups jointly reported that tracking dynamics of single urease is feasible beyond the diffraction limit (24). Extra care was taken by adding polymeric solution to ensure that the enzyme does not stick to the cover glass and also to restrict the movement of enzymes to two dimensions (**Figure 1*c***). The trajectories of the catalytically active urease were followed by recording snapshots at 20 frames/s; the increase in diffusion coefficient was found to be several-fold higher than that reported earlier by Muddana et al. (**Figure 1*d–f***). Haw and coworkers fabricated biohybrid systems made of alkaline-phosphatase-conjugated quantum dots and tracked their diffusion by customary fluorescence microscopy. The hybrid particles displayed enhanced diffusion only when the micellar substrate was converted to fibrils and remained unaffected when aggregated structures were formed (44).

Dey et al. exploited the force from enzyme catalysis to propel microparticles (2). In this work, spherical polystyrene (PS) microparticles with attached urease and catalase enzymes displayed enhanced motion when their diffusive behavior was studied with dynamic light scattering (DLS). The enzyme-powered micromotors showed ∼40% enhancement in diffusion when the substrate was added. Sanchez and coworkers used a combination of optical microscopy, MSD analysis, and DLS experiments to account for the self-propulsion of enzyme-powered nanomotors made of submicron-sized Janus silica particles covalently tagged with three separate enzymes: urease, glucose oxidase (GOx), and catalase (3). All the nanomotors displayed diffusion enhancement in the range of 35–85% at saturating substrate concentration, and the force associated with such catalytically powered motion was estimated using optical tweezers. Interestingly, the self-propulsive behavior of these nanomotors was found to be dependent on the k_{cat} value of the enzyme (**Figure 2*c–e***) (41). In contrast to fluorescence or other optical techniques, Jiang et al. used nonconventional electrochemical-based cyclic voltammetry technique to demonstrate the previously reported enhanced diffusion of catalase with H_2O_2. They observed an increase in the collision frequency between the diamond electrode and the catalase molecule during the catalytic reaction due to an electron transfer mechanism, which was correlated to the increase in diffusion as seen with FCS (45). In another work, magnetic micropropellers made of silica and Ni particles utilized the mechanical force from immobilized urease during catalysis to show enhanced diffusion across gastric mucin gels. The study used optical microscopy and a fixed magnetic field to track the motion of the micropropellers (27). Patiño et al. have shown that when urease enzyme is coated on PS or on PS coated with SiO_2-shell (PS@SiO2) beads, the inherent asymmetries in enzyme attachment lead to higher propulsion (46). Although they used optical microscopy–based direct tracking methods to determine the self-propulsion behavior of the beads, high-resolution stochastic optical

reconstruction microscopy (STORM) was employed to quantify the asymmetries and amount of enzyme on the enzyme-coated beads.

Phoresis: a surface force–driven motion due to concentration gradients of ionic or neutral species around the particle

2.4. Possible Mechanism for Enhanced Diffusion

Understanding the precise mechanism behind catalysis-induced enhanced diffusion of enzymes is a long-standing challenge due to the complexity in their dynamics and differences in the behavior of each enzyme in the molecular regime. Nevertheless, some of the recent studies have suggested plausible mechanisms to account for the experimental observations (6, 12, 47).

2.4.1. Phoretic mechanism of enhanced diffusion. Phoresis is an important mechanism responsible for the directed or stochastic motion of active species undergoing chemical reaction (28). Enzymes are also assumed to adopt similar means while exhibiting enhanced motion. A typical example is urease, which converts urea to ammonium and bicarbonate ions. This catalytic conversion from neutral to ionic species imposes a self-generated local electric field in the vicinity of the enzyme, which imparts a force on the enzyme because of the difference in diffusivities of the anion and cation. Hence, the freely dispersed urease shows propulsion until the charged species diffuse away into the bulk solution (23). The same mechanism is not anticipated for other enzymes like DNA and RNA polymerase or catalase, which also show enhanced diffusion but convert their substrates into nonionic products. DNA or RNA polymerase catalyzes nucleotide triphosphates (NTPs) to their corresponding monophosphates during complex formation with DNA template, whereas catalase initiates the disproportionation of H_2O_2 into water and oxygen (1, 31, 48). The question of how enhanced diffusion can be interpreted as a phoretic process for these enzymes remains unresolved. Golestanian and coworkers have proposed that reactions involving neutral molecules may also generate local concentration gradients near the enzyme active site due to asymmetric distribution of reactant and product molecules that causes diffusiophoretic motion of the enzyme (49). The direction of the movement is controlled by the interaction strength of the enzyme with the reactant and product molecules and subsequent gradient formation. However, the phoretic mechanism is still considered trivial because the size of enzymes typically lies in the range of a few nanometers, and they exhibit very fast rotational diffusion times (10^{-6} s). In that short timescale, enzymes might not be able to sense the orientational information generated by the asymmetric catalytic turnover before Brownian randomization takes over (6, 12).

2.4.2. Enhanced diffusion due to thermal effects. In 2014, Bustamante and coworkers performed FCS experiments with four different enzymes with their respective substrates to understand the mechanistic relation between enhanced diffusion and the heat change associated with the catalytic reaction (50). The study involved urease, catalase, and alkaline phosphatase, which catalyzes exothermic reactions with enthalpy changes (ΔH) ranging between -45 and -100 kJ/mol. In addition, they also studied the diffusion of triose phosphate isomerase enzyme, which is thermoneutral with a value of $\Delta H = -3$ kJ/mol. Interestingly, only the exothermic enzymes displayed enhanced diffusion (30–80%) in the presence of their substrate. The authors proposed that the heat released during catalytic turnover produced a differential stress at the enzyme–solvent interface in the form of an asymmetric pressure wave that transiently displaces the center-of-mass of the enzyme in response to the stress. Furthermore, by computational analysis, they estimated the acoustic pressure on the solvent exerted by the expanding enzyme to be about 500 pN/nm^2, which translates to a value of ~10 pN force/catalytic turnover for an enzyme roughly 10 nm in size. This result agrees well with the simulations reported by Butler et al. (12). However, rapid heat transfer to the surrounding solvent or energy redistribution within the molecule at an ultrafast timescale was completely ignored (51). Golestanian carried out calculations and explored

the plausible mechanism involving local heat effects proposed by Riedel et al. It was found that the thermal effect was too small to contribute to the enhanced diffusion of enzymes. Rather, Golestanian proposed that the combination of global heat increase of the sample container and decrease in viscosity and conformational changes of the enzyme are collectively responsible for the enhanced diffusion of exothermic enzymes (52). Experimentally, Dey et al. were first to report that a catalytic reaction involving urease and urea resulted in only a 0.2-K increase in temperature when measured with a thermocouple in a nuclear magnetic resonance (NMR) spectroscopy experiment (2). Such a small rise in temperature should not induce any diffusion change of the enzyme in accordance with the theory predicted by Golestanian. Furthermore, FCS study of a catalytic reaction involving aldolase with substrate FBP showed an ∼30% enhancement in diffusion coefficient despite the reaction being endothermic with $\Delta H = 60$ kJ/mol (32). However, the enhanced diffusion of aldolase was not observed when monitored by DLS and NMR (53, 54). Overall, thermal dependence of enhanced diffusion of enzymes seems uncertain as a plausible mechanism.

2.4.3. Conformational change–mediated enhanced diffusion. Conformational change of the enzyme is another plausible mechanism for enhanced diffusion. Kapral and others proposed that enhanced enzyme diffusion occurs via nonreversible changes in enzyme conformation upon substrate binding and product formation, resulting in asymmetric fluid fluctuations as the driving force (20, 55). Reversible conformational changes were not considered for enzyme propulsion because in that case a net displacement would not occur with respect to initial position according to the Scallop theorem (11). They followed up with another study showing an active molecular swimmer binding a substrate would result in net free energy change, causing a conformational change (56). Based on the FCS study of aldolase, Illien et al. (32) framed enhanced diffusion in terms of reversible binding–induced conformational fluctuations of the enzyme. The dumbbell-shaped aldolase was assumed to behave like a spring that undergoes structural changes upon binding and/or unbinding with reactant molecules that leads to its motion. They also proposed a model considering the stochastic switching between the two equilibrium states (free and bound) of the enzyme. The diffusion change was expressed as: $\frac{\Delta D}{D_0} = \alpha \frac{[S]}{K+[S]}$ where α is a dimensionless coefficient that varies with the shape changes and internal degrees of freedom of aldolase upon reversible binding, S is the concentration of reacting molecule, and K is the equilibrium binding constant. Hence, diffusion of an enzyme that is hydrodynamically coupled to its surrounding is expected to increase in a reactant concentration–dependent manner exhibiting Michaelis–Menten-like characteristics but independent of catalytic turnover. In another study by Minteer and coworkers, an enzyme cascade comprising malate dehydrogenase and citrate synthase showed enhanced diffusion under catalytic conditions and also with just the cofactors present (30). These findings confirmed that catalysis is not essential for observing enhanced motion for enzymes. However, some of the recent reports suggest that diffusion changes might be a consequence of enzyme dissociation upon substrate binding or inherent issues with the sensitivity of the methods used for recording diffusion processes (36, 47, 53, 54, 57). Therefore, in addition to experimental observation of enhanced diffusion, the theoretical interpretation of the phenomenon is also important for its generalization and detailed mechanistic understanding.

2.5. Theoretical Interpretation of Enhanced Diffusion

Enhanced diffusion arises from impulsive force generated when substrates are converted into products by enzymes, which is reflected as an increase in the enzymes' mechanical motion. Theoretical calculations and simulations suggest that the magnitude of the force is comparable with that produced by motor proteins.

2.5.1. Impulsive force from catalytically active enzymes. Butler et al. used Langevin dynamics simulations to evaluate the theoretical impulsive force generated by the enzyme during catalytic turnover (12). The simulation was performed by applying a fixed force for a time that corresponds to the reaction rate of the enzyme; additionally, a drag coefficient ensured that the enzyme motion is not spatially infinite. For each enzyme, the simulation trajectories were obtained for more than 50 molecules in buffer (or substrate) for a total run time of 0.1 s and integration step of 10 ns. MSD against time interval was plotted to obtain the diffusion coefficient from the slope. During each successive simulation step, the force per catalytic turnover was adjusted until the simulated diffusion coefficient, which was enhanced in the presence of substrate, overlapped with the experimentally obtained value. Taking urease and catalase as model enzymes, the force per reaction turnover was estimated to be 12 and 9 pN/catalytic turnover, respectively. These values are exceptionally close to the experimentally calculated forces (5–10 pN) that act during each stepping motion of polymerases and motor proteins (19, 58–60).

2.5.2. Proposed theoretical models for enhanced diffusion. One of the earliest theories relates enzyme self-propulsion to asymmetric distribution of products. By applying molecular dynamics simulation on a model dimer motor in a solvent, Colberg & Kapral claimed that the products that are formed interact asymmetrically with the active site of the dimer through their Lennard–Jones potential (61). The inhomogeneous concentration gradient that builds up can propel the motor whose direction and rate are controlled by product and solvent characteristics. In another study, Golestanian proposed a minimal kinetic model for a molecular swimmer that undergoes nonreciprocal conformation changes to display mechanochemical propulsion (62). This is the first theory on swimmers working at low Reynolds number that can be extended to enzymes or motor proteins showing enhanced diffusion. However, the author stressed that the randomization of the swimmer orientation from thermal fluctuations and the rotational diffusion occurring at fast timescales would cause the diffusion changes to be too small for precise determination. A similar idea was presented in another work, where enzyme motility was attributed to the interplay between the energy landscape and the hydrodynamic coupling to the surrounding environment (37). Based on analysis of their diffusing enzyme model, the authors suggested that stroke size from the enzyme is limited to its hydrodynamic length, which makes diffusion changes quite small in value.

Mikhailov & Kapral suggested in a simple model that hydrodynamic collective effects play a role in enhancing the diffusion of enzymes in biological environments like membranes in which the concentration is high (20). A crowded environment can also influence the hydrodynamic effects owing to active force dipoles enhancing diffusion constants substantially. They tested model lipid bilayers and found the effects are strongly nonlocal, so that active inclusions in the entire membrane contribute to local diffusion enhancement and the chemotaxis-like drift due to gradients of active proteins present. By performing a molecular dynamics simulation on a model dumbbell-shaped active molecule that stochastically changes between open and closed states upon substrate binding, Dennison et al. validated enhancement in enzyme diffusion whose magnitude is regulated by the system parameters and solvent properties (55). Feng & Gilson investigated enzyme diffusion through kinematic and thermodynamic theoretical models without biasing toward any specific propulsion mechanism (63). Compiling kinetic as well as thermodynamic data for several enzymes studied previously, they concluded that the propulsion speed corresponding to experimental values of enhanced diffusion cannot be attained through simple conversion of chemical energy from catalytic turnover. According to Lauga, for enzyme motion at low Reynolds number, the coupling of Brownian randomization and reciprocal motion will lead to net displacement and increased diffusivities (64). The fluctuating dumbbell model of enzymes proposed by Illien et al. was revisited by Kondrat & Popescu applying Brownian dynamics simulations. They

verified the enhancement in diffusion due to enzyme size fluctuation upon substrate or inhibitor binding but suggested that the effect of hydrodynamic coupling does have an impact in the enhancement process (65). Granick and coworkers supported experimentally observed enzyme leaps during catalysis through a simple model. According to this model, the enzyme is propelled by an episodic catalytically driven boost of 1 pN that exists for 6 μs to overcome the rotational randomization, finally moving the enzyme ballistically over a distance of about 50 nm against the viscous drag (66). The Sanchez group applied molecular dynamics simulations to show that conformational dynamics of enzymes play a vital role in the propulsion of enzyme-attached microcapsules (41). When analyzing the simulation results, they observed that fast enzymes like urease and acetylcholine esterase possess greater flexibility near the active site compared to slower enzymes like GOx and aldolase. Thus, the majority of the recent theoretical work suggests that enhanced diffusion of enzymes varies with the substrate concentration in agreement with experimentally observed Michaelis-Menten-like dependence (67, 68).

Janus particle: has two faces on opposite sides that can be functionalized independently

Protocells: model structures primarily composed of spherical assemblies of lipids, polymers, and/or proteins that mimic aspects of living cells

3. CHEMOTAXIS OF ENZYMES AND ENZYME-ATTACHED COLLOIDS

3.1. Experimental Work on Enzyme Chemotaxis

Directional migration in response to specific signals is critical for the survival of living systems. Chemotaxis (the movement toward or away from chemical stimuli) enables living cells to move toward food or escape away from toxins, exchange chemical signals with the environment, transport cargo, and coordinate collective behavior such as biofilm formation and tissue development (69, 70). Given its high importance and ubiquity in living systems, the question is can we mimic the same behavior in vitro, to parallel cellular chemotaxis? This will not only enable us to determine the various types and mechanisms of chemotaxis but also have relevance in the development of cellular models and/or efficient drug delivery systems through chemotaxis.

3.1.1. Chemotaxis of single-enzyme molecules. Chemotaxis has been observed in synthetic, nonliving systems such as Janus particles and in biologically relevant systems such as enzymes and protocells (1, 2, 71). One of the first experimental studies to demonstrate chemotaxis of biomolecules in vitro was done by Schwartz and coworkers (48). In this study, they demonstrated the chemotactic movement of a complex containing DNA and its associated RNA polymerase driven by the transcription substrate, NTPs. Another study from the Sen group showed that single-enzyme molecules such as urease and catalase, when placed in gradients of their reactants, show directional migration toward higher concentrations upon catalytic turnover; this is also a form of molecular chemotaxis (**Figure 3*a*,*c***) (1, 72). They employed a two-inlet-one-outlet microfluidic device in which the fluorescently tagged enzymes were flown through one inlet while buffer and reactant for the enzyme were flown through the other inlet. In another study, the Sen group also showed that DNA polymerase can function as a motor and moves toward a higher concentration of substrate and cofactor (31). The phenomenon of chemotaxis has been observed with single-enzyme molecules (1) and multienzyme cascades with sequential chemotaxis toward the initial substrate (29), as well as enzyme-coated hard (2) and soft particles (71). To demonstrate the efficacy of chemotaxis in cellular cascade reactions, the coordinated and interdependent movement of the first four enzymes in the glycolysis cycle were studied: hexokinase, phosphoglucose isomerase, phosphofructokinase, and aldolase (29). In this study, it was demonstrated that each enzyme moved chemotactically up its individual reactant gradient that was produced by the preceding enzymatic reaction. For this study, a three-inlet-one-outlet microfluidic device was employed (**Figure 3*b***). By precisely specifying the flow rates and channel dimensions, the diffusion time and

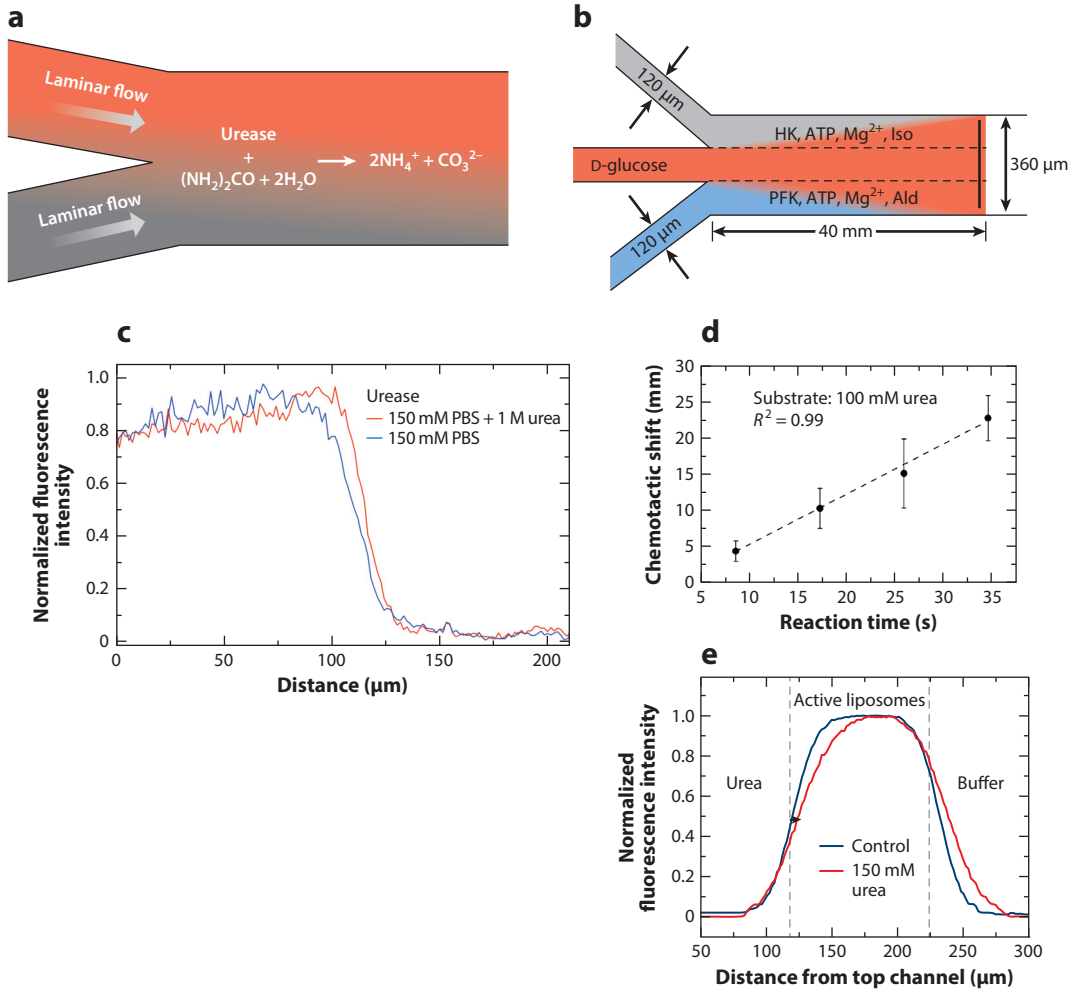

Figure 3

(*a*) Schematic of a two-inlet-one-outlet Y-shaped microfluidic device. (*b*) Schematic of a three-inlet-one-outlet microfluidic device. (*c*) Plot of the mean normalized fluorescence intensity profile as a function of lateral position along the width of the channel, which showed a shift for urease toward 1 M of urea in 150 mM of PBS buffer (*red*), as compared to toward 150 mM of PBS buffer (*blue*), when viewed under a confocal microscope. (*d*) Chemotactic migrations of urease-coated microparticles measured at different times (at different positions of the microfluidic channel along its length, from the start) at 100 mM of urea. (*e*) Fluorescence intensity profiles of urease-coated liposomes in imposed gradients of urea. The arrow in panel *e* indicates that the active urease-coated liposomes move away from the substrate (negative chemotaxis), with [urea] = 150 mM, [phosphate buffer] = 100 mM. Panels *a* and *c* adapted with permission from Reference 1; copyright 2013 American Chemical Society. Panel *b* adapted with permission from Reference 29; copyright 2018 Springer Nature. Panel *d* adapted with permission from Reference 2; copyright 2015 American Chemical Society. Panel *e* adapted with permission from Reference 71; copyright 2019 Springer Nature. Abbreviations: ATP, adenosine triphosphate; Ald, aldolase; HK, hexokinase; Iso, isomerase; PBS, phosphate buffered saline; PFK, phosphofructokinase.

interaction time between the enzyme and substrates can be controlled. Optical scans were taken across the channel width at a distance of 38 mm from the inlet (~34-s residence time) using a confocal laser scanning microscope. Chemotactic shifts of enzymes were measured perpendicular to the direction of flow. Additionally, the formation of aggregates of the four enzymes was observed, demonstrating the possibility of chemotaxis as a potential mechanism for metabolon formation

in living systems. This substrate-dependent chemotactic assembly was demonstrated not only in simple buffers but also under conditions that mimic cytosolic crowding.

In contrast to previous findings, Granick's group has recently reported that urease and acetylcholine esterase enzymes move spontaneously down a gradient of their respective substrates (antichemotaxis) by a process that is similar to the run-and-tumble strategy of microorganisms (43). In this study, they used STED-FCS to study enzyme chemotaxis through subdiffraction-sized spots in both diffusive and ballistic modes of propulsion.

Liposomes: vesicles made of lipids

Polymersomes: vesicles made of polymers

Stomatocytes: bowl-shaped soft containers with an opening on one side that enables communication between the inside space and the external environment

3.1.2. Chemotaxis of enzyme-attached or -encapsulated soft particles. In recent years, soft colloids such as liposomes (40, 71) and polymersomes (73–76) have come under the spotlight as potential self-propelled motors or cargo delivery vehicles due to their high biocompatibility and structural mimicry of the membranes present in natural cells. The movement of soft colloids in imposed gradients have been described both experimentally and theoretically, where the asymmetry for propulsion is provided by the surrounding environment (77–80). However, self-propulsion of soft colloids due to catalytic turnover have been more recently demonstrated. To understand how inanimate systems can transition into living matter, scientists around the world have developed systems that mimic the design rules of compartmentalization and/or molecular crowding as seen in living systems (81). As such, protocells that are capable of multicompartmentalization, membrane growth, reproduction and division, and predatory behavior have been studied (82, 83). However, the ability to incorporate dynamic and autonomous properties into these protocells remains a challenge. Protocell motors with catalysts in a confined environment such as on the surface, at an interface, or inside a small volume have been fabricated in recent years. One of the first studies to show chemotactic movement of polymer stomatocytes was by the Wilson group. They described the enhanced diffusion of platinum (Pt)-encapsulated polymer stomatocytes and subsequently demonstrated the ability of these Pt-laden polymer stomatocytes to show directed motion toward higher concentrations of their reactant, H_2O_2 (73, 74). This behavior was shown using a two-inlet-one-outlet channel as described previously (**Figure 4*a***). These Pt-laden stomatocytes, which also encapsulated a model drug, were also shown to move toward H_2O_2-secreting neutrophil cells, demonstrating a potential application of drug delivery (74).

Moving to enzyme catalysis, the next study focused on encapsulating catalase and GOx inside the polymer stomatocytes and studying their motile behavior. The Wilson group measured the increased propulsion of both one-enzyme (catalase only) and two-enzyme (catalase and GOx) systems through nanoparticle tracking analysis (75). A similar study was conducted by the Battaglia group in which asymmetric polymersomes encapsulating GOx and catalase enzymes exhibited positive chemotaxis in a gradient of the initial substrate, D-glucose (**Figure 4*c***) (76). Using a slightly different configuration, the Hammer group fabricated biotinylated polymersomes that encapsulated catalase and adhered them weakly to an avidin-coated surface (**Figure 4*b***; 84). Upon catalytic turnover when exposed to H_2O_2, a differential impulsive force is generated that can break and reform the avidin-biotin bonds, leading to a random motility–mimicking diffusive motion. In a more recent study from the Sen group, soft motors that differed from the above in two respects were designed (71). First, the soft particle used was a liposome. Liposomes are self-assembled systems whose main structural component is phospholipids. Phospholipids are particularly attractive due to their structural similarity to cell membranes in living systems and high biocompatibility and bioavailability. Second, enzymes were attached on the external surface of the liposomes through biotin–streptavidin conjugation. Here, positive chemotaxis of catalase-coated liposomes, negative chemotaxis of urease-coated liposomes, and tunable chemotaxis of ATPase-tagged liposomes were demonstrated. What was surprising was that even though single urease molecules and urease-coated PS particles show positive chemotaxis, the same enzyme when attached to a

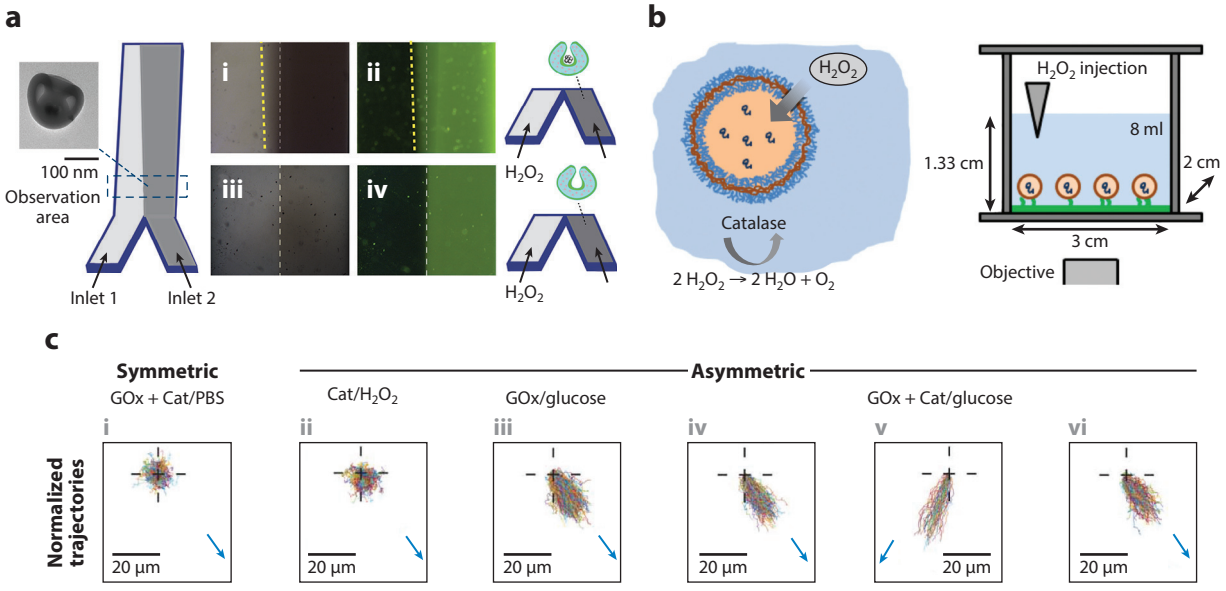

Figure 4

(*a*) Chemotaxis evaluation in a two-inlet-one-outlet microfluidic channel. Lateral shifts of Dox- and Pt nanoparticle–loaded stomatocytes in the presence of 0.05% H_2O_2: (*i*) bright field and (*ii*) fluorescent image. No deviation toward the fuel of the only Dox-loaded stomatocytes in presence of 0.05% H_2O_2: (*iii*) bright field and (*iv*) fluorescent image. (*b*) Biotinylated polymersomes encapsulating Cat are dispersed in a custom-made experimental chamber. The bottom of the chamber is coated with a low density of avidin. The polymersomes weakly adhere to the chamber bottom. A small volume (0.1 mL) of either 3 or 30 wt% H_2O_2 is injected into the chamber; H_2O_2 passes through the membrane and is converted by Cat in the polymersome lumen, generating force and motion. (*c*) (*i*) Symmetric PMPC-PDPA polymersomes loaded with GOx and Cat responding to a glucose gradient; (*ii*) asymmetric PMPC-PDPA/PEO-PBO polymersomes loaded with Cat and responding to a hydrogen peroxide gradient; (*iii*) asymmetric PMPC-PDPA/PEO-PBO polymersomes loaded with GOx and responding to a glucose gradient; (*iv*,*v*) asymmetric PMPC-PDPA/PEO-PBO polymersomes loaded with GOx and Cat responding to a glucose gradient coming from the (*iv*) right-hand side and (*v*) left-hand side; and (*vi*) asymmetric POEGMA-PDPA/PEO-PBO polymersomes loaded with GOx and Cat responding to a glucose gradient coming from the right-hand side. Blue arrows indicate the direction of the substrate gradient. Panel *a* adapted with permission from Reference 74; copyright 2015 Wiley-VCH. Panel *b* adapted with permission from Reference 84; copyright 2018 Wiley-VCH. Panel *c* adapted with permission from Reference 76; copyright 2017 American Association for the Advancement of Science (AAAS). Abbreviations: Cat, catalase; Dox, Doxorubicin; GOx, glucose oxidase; PBS, Phosphate Buffered Saline; PEO-PBO, poly(ethylene oxide)-poly(butylene oxide; PMPC-PDPA, poly[(2-methacryloyl)ethyl phosphorylcholine]–poly[2-(diisopropylamino)ethyl methacrylate].

liposome surface showed negative chemotaxis (**Figure 3*e***). Ruling out transport of liposomes due to electrolyte-diffusiophoresis, osmophoresis, and density-driven flows, a previously unrecognized mechanism of motion for negative chemotaxis was hypothesized. Solutes can interact with the surface of liposomes through excluded volume effects, dipole interactions, ion pairing interactions, or van der Waals forces (85). The Hofmeister series is a classification of anions and cations according to their ability to salt-out (aggregate or precipitate) or salt-in (solubilize) organic molecules and biomolecules. Ions and neutral osmolytes (such as carbonate and sulfate ions, and glucose) that are hydrated do not associate well with hydrophobic organic molecules and biomolecules, and repel them. Thus, the products of the urease reaction, ammonium and bicarbonate ions, repel the urease-coated liposomes, resulting in negative chemotaxis.

3.1.3. Potential applications of enzyme chemotaxis. The chemotactic migration of active enzymes toward higher concentrations of reactant has also been used to demonstrate practical

applications such as the separation of active and inactive enzymes from a mixture (86). Using a microchannel network, when a mixture of fluorescently tagged active and inactive enzymes were flown in a gradient of substrate, active enzymes were seen to move toward the channel containing the substrate, allowing for a simple separation of inactive and active enzymes. Furthermore, methods that do not rely on fluidic devices, such as paper-based chemotactic separation of enzymes, have also been developed (87). A potential application of chemotaxis is the delivery of passive cargo by attaching enzymes to the cargo. This has been demonstrated by attaching enzymes (catalase and urease) to PS microparticles and subjecting them to gradients of their respective reactants (2). The extent of chemotaxis is proportional to the exposure time to the substrate (**Figure 3*d***). The enzymes were attached onto the PS beads through biotin–streptavidin conjugation.

3.2. Theory of Chemotaxis

Understanding the mechanism of chemotaxis would be beneficial in predicting motile behavior for potential applications such as cargo delivery and/or environmental remediation. A comprehensive theoretical description of gradient-sensing by Janus particles, leading to chemotactic or antichemotactic behavior, was put forth by Saha et al. (88). Schurr et al. proposed a theory for chemotaxis that explained the thermodynamic tendency of macromolecules to move up the concentration gradient of a binding substrate in solution (89). In another work, the Hess group predicted that in a gradient of stationary binding sites, macromolecules would move toward regions of higher density of binding sites. Hence, binding lies behind the thermodynamic origin of molecular chemotaxis (90, 91).

As a modification of Schurr's theory, a model describing the chemotactic behavior of active enzymes based on substrate binding–unbinding was proposed (29, 72). According to this hypothesis, chemotactic shift arises from a thermodynamic driving force that lowers the chemical potential of the system due to favorable substrate binding. The substrate gradient-induced enzyme chemotaxis by cross-diffusion is in the opposite direction to Fickian diffusion, transferring enzymes toward regions of higher substrate concentration. The diffusive flow for the concentration c_e of enzyme, e, in the presence of its substrate, s, can be written as

$$J_e = -D\nabla c_e - D_{XD}\nabla c_s, \qquad 1.$$

where D is the Brownian diffusion coefficient of enzyme, D_{XD} is the cross-diffusion coefficient, and ∇c_e and ∇c_s are gradients in enzyme and substrate concentrations, respectively. The cross-diffusion coefficient, D_{XD}, is a function of the local substrate concentration, c_s, the diffusion coefficient, D, and the equilibrium constant, K, for substrate binding to the enzyme:

$$D_{XD} = -Dc_e\frac{K}{1+Kc_s}. \qquad 2.$$

Combining these two equations gives

$$J_e = -D\left(\nabla c_e - c_e\frac{K}{1+Kc_s}\nabla c_s\right). \qquad 3.$$

This equation highlights the factors that drive cross-diffusion flux. The first term inside the parentheses is the diffusive flux toward lower concentrations of enzyme. The second term is the chemotactic flux of the enzyme, which has the opposite sign, showing that this flux is toward higher concentrations of substrate. In addition to the substrate gradient, this term's magnitude is determined by the diffusion coefficient, D and the enzyme concentration. The proposed model involving binding-induced cross-diffusion has no adjustable parameters. Furthermore, changes in enzyme diffusion affect the magnitude but not the direction of the cross-diffusion flux and predicts the occurrence of chemotaxis for favorable binding interaction between any two molecular

species. As the above analysis suggests, all molecules will chemotax up a gradient of an attractant, depending on the interaction and concentration gradients. The chemotaxis mechanism often gives transport rates several times that of diffusion. This fact, combined with its directionality, can make chemotaxis a valuable strategy for transport over longer distances.

In another theoretical work, it was hypothesized that enzyme chemotaxis could be the net result of two competing phenomena of phoretic motion due to nonspecific interactions and substrate binding–unbinding (67). However, the Sen group have shown that hexokinase chemotaxes toward D-glucose but not L-glucose; i.e., without specific binding interaction there is no chemotaxis (neither positive nor negative), though nonspecific interactions could still exist (29, 72).

4. PUMPING BEHAVIOR OF ACTIVE ENZYMES

When active enzymes are fixed in place, they can transfer the catalytically generated force to the surrounding fluid and move the fluid, as well as any particles that are suspended in it. Typically, enzymes are attached to a surface patch via either electrostatic interactions or biotin–streptavidin linkages (**Figure 5*a***; 25, 94, 95). More recent are bioinorganic hybrid pumps, which have enzymes attached to a bacteriophage that is in turn attached to an inorganic metal particle (93). Regardless of the method by which enzymes are immobilized on a fixed surface, when in a closed system and subject to the substrate of the enzyme, they generate convective motion of the surrounding fluid. The convective nature of the fluid is quantified by adding in tracer particles to the system and watching them move directionally. Depending on the type of enzyme used and concentration of reactant, the directionality and speed of pumping can be controlled. For example, catalase, GOx, and lipase pump fluid inward (i.e., particles are pumped toward the enzyme patch on the surface) and urease pumps fluid outward (i.e., particles are pumped away from the enzyme patch on the surface). Due to fluid continuity, the fluid flow is reversed when viewed above the enzyme-patterned surface. The difference in fluid pumping directions among different enzymes was hypothesized to be due to the differences in densities between the reactants and products of the enzymes. This was confirmed by inverting the pump setup and observing a reversal in the direction of fluid flow. Additionally, thermal buoyancy due to exothermicity of the enzymatic reaction was ruled out as a dominant mechanism by comparing experimental pumping values with theoretical pumping values obtained from modeling (95, 96). Having enzymes immobilized on a surface constitutes a unique geometry and a platform that combines microscale pumping with sensing for potential applications. In one of the first demonstrations of enzyme pumps, the Sen group demonstrated the controllable release of insulin from a gel that also had GOx embedded in it (**Figure 5*b***) (25). As the enzyme-attached gel encountered the reactant glucose in the surrounding fluid, it was able to pump out insulin in response. The insulin release rate depended on the concentration of glucose in the ambient, making it a potential insulin delivery pump. In another example, sensors for toxic substances such as mercury, cadmium, cyanide, and azide were designed with the help of catalase and urease pumps (94). From the attenuation of pumping speed, the concentration of the toxic substance can be determined with detection limits well below the concentrations permitted by the Environmental Protection Agency. In another publication by the Fischer group, bacteriophages were used as biological templates for enzyme immobilization, which were in turn attached to an inorganic support making it a bioinorganic hybrid construct (**Figure 5*d***) (93). In that paper, they demonstrated the feasibility of such a construct using urease as an example. Using a biological template for the immobilized enzymes helped to retain the activity of the enzymes, which may otherwise be reduced when they are directly linked to inorganic substrate as seen in previous studies. Having a modular approach,

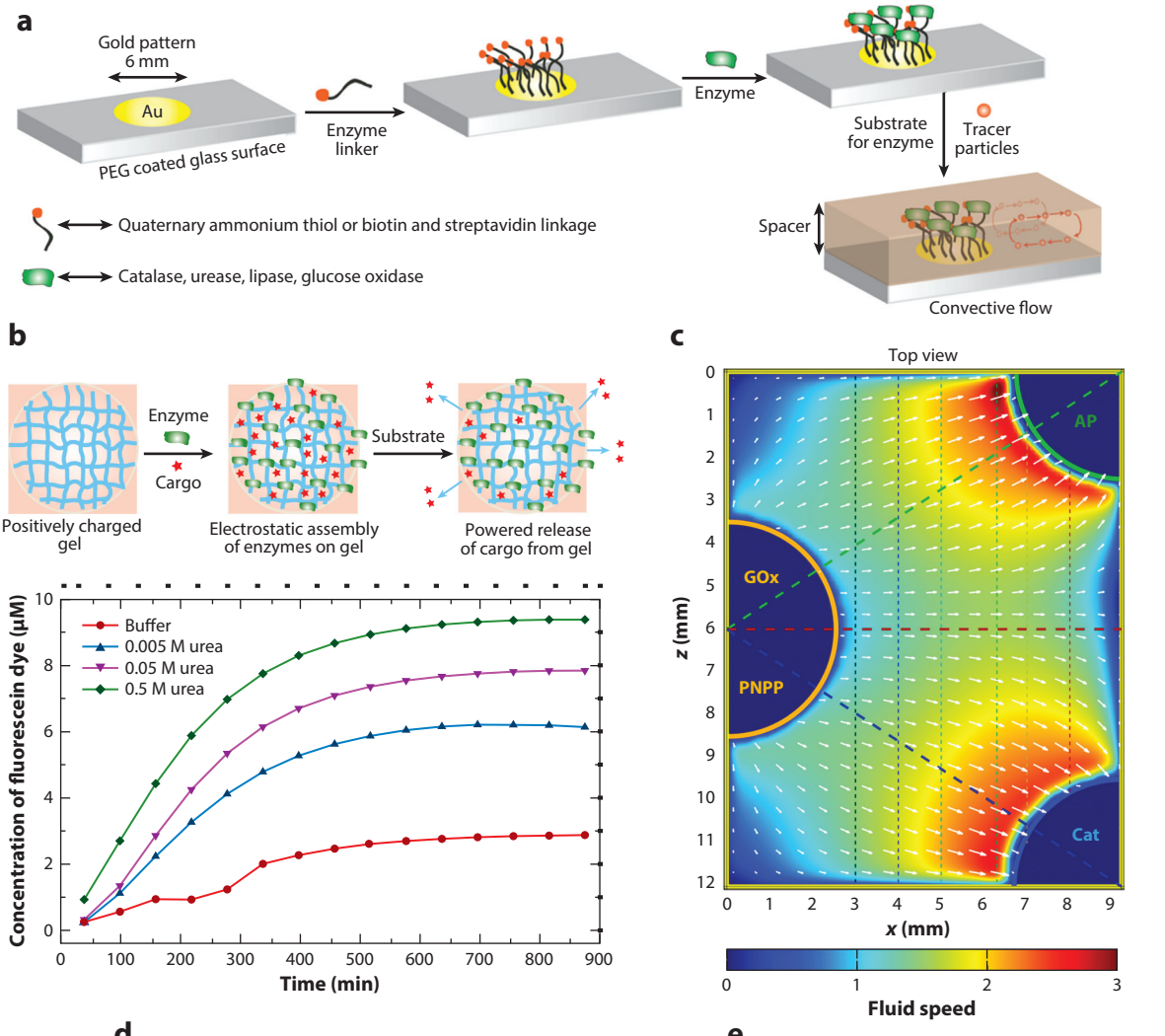

(*Caption appears on following page*)

Figure 5 (*Figure appears on preceding page*)

Pumping behavior of active enzymes. (*a*) Schematic of the enzyme-powered micropump immobilization procedure and triggered fluid pumping in the presence of substrate. (*b*) A general schematic that shows the functionalization of enzyme molecules on a positively charged (quaternary-ammonium-terminated) hydrogel, followed by the triggered release of cargo in the presence of the enzyme substrate. The concentration of dye (fluorescein) molecules released from urease-anchored hydrogel as a function of time in the presence of different concentrations of urea, monitored using a UV–vis spectrophotometer. The profile shows an increase in the amount of dye released from the hydrogel with increasing urea concentration. (*c*) The color map of horizontal fluid velocities illustrates bifurcating fluid flow directed from P_{GOx} to P_{Cat} and from P_{GOx} to P_{AP}, emphasized by yellow-to-red transitions. The magnitude of fluid velocities in micrometers per second is shown by the color bar and directions by white arrows. (*d*) The E–P–Cs (*brown*) are attracted to the bottom surface of the chamber by a small permanent magnet. The orange arrows indicate the direction of the fluid flow after the addition of urea. (*e*) Average convective flow speeds measured in blood samples. The E–P–C constructs are functional in this complex medium, where the red blood cells act as tracer particles and the urea concentration found in blood is sufficient for powering the system. Inset: Red blood cells in the micropump setup. Panel *a* adapted with permission from Reference 6; copyright 2018 American Chemical Society. Panel *b* adapted with permission from Reference 25; copyright 2014 Springer Nature. Panel *c* adapted with permission from Reference 92; copyright 2019 American Chemical Society. Panels *d* and *e* adapted with permission from Reference 93; copyright 2019 American Chemical Society. Abbreviations: AP, acid phosphatase; Cat, catalase; E–P–C, enzyme–phage–colloid; GOx, glucose oxidase; PEG, polyethylene glycol; PNPP, p-nitrophenyl phosphate.

the system exploits the advantages of each component. Furthermore, the viability of this hybrid micropump was shown under physiological conditions utilizing urea from blood (**Figure 5*e***).

Directed transport of microparticles is another potential application that has been demonstrated using enzyme micropump systems (97). Due to fluid density gradients formed upon catalysis, induced convective flow carries the suspended target particles and deposits them at a specific position on the surface. The velocity and peak cargo particle density location can be tuned. Furthermore, the process can be repeated by introducing fresh reagent into the microchamber. Self-organization of fluid has also been demonstrated by utilizing a cascade of enzyme pumps (**Figure 5*c***; 92). Three enzymes, GOx, catalase, and acid phosphatase, incorporated into separate gels have been exploited to control the temporal interactions between three pumps in a triangular arrangement. The spatiotemporal interactions among the chemical reactions produce well-defined fluid streams, which transport chemicals and form a fluidic circuit. The layout and flow direction of each fluid stream can be controlled through the number and placement of the gels and the enzymes localized in the gels. These studies provide a new method for designing self-organizing and bifurcating fluids that can provide fundamental insight into nonequilibrium, dynamical systems. As the flow circuits are generated by internal chemical reactions, the fluid can autonomously transport cargo to specific locations in the device. In addition to experimental demonstrations of enzyme micropumps, there have been several theoretical studies focusing on increasing complexity of enzyme micropumps from single-enzyme pumps to multiple-enzyme pumps that are either unrelated or related to each other through cascade reactions. Some of these studies have also focused on different designs of enzyme patches (apart from the traditional round patches used in experiments), such as enzyme-coated flexible sheets resembling a crab with distinct claws (98). This allows for additional degrees of movement, resulting in the development of more complex fluid flows in enzyme pump systems. These theoretical models not only expand the applicability of enzyme micropumps but also have the potential to lead to the field of enzyme-coated soft robotics.

5. HARNESSING ENZYME MOTION FOR BIOLOGICAL FUNCTIONS

5.1. Role of Enzymatic Forces in Cellular Processes

The cell contains a vast array of enzymes located in either the plasma membrane or the cytoplasm and each of them participates in different tasks that collectively and coherently contribute

to the proper functioning of the cell. Several of these enzymes such as kinesin and dynein serve as molecular motors to transport cargo (99). Others, like transmembrane ATPases, play a vital role in signaling and ion balance (100). Most of these enzymes are powered by the hydrolysis of ATP to ADP and phosphate, during which they undergo conformational fluctuations to adapt to the surrounding changes (12). A classic example is the random walk of kinesin motors on microtubules (15). Eventually they generate force fluctuations that drive critical functions of the cell such as division, migration, and contraction (101). Butler et al. pointed out that forces produced by freely dispersed enzymes during catalysis are adequate to activate biomolecules that take part in cellular sensing and may lead to stochastic pulsing and convection of cytoplasmic fluid (12). The structural fluctuations in cellular enzymes, resulting from collective force generation, can also induce cell migration, breakdown of cell–cell junctions, or deformation in cell shape (102). Guo et al. used force-spectrum-microscopy to quantify such forces acting inside the cytoplasm and its role in the regulation of the stochastic motor activity (103). Interestingly from the study, the estimated frequency range of the stochastic fluctuations in the cytoplasm was found to be 10^{-1}–10^{2} s^{-1}, which complements the turnover number reported for several freely dispersed enzymes very well.

The formation of metabolons involving enzymes in a cascade is an example of collective behavior at the molecular scale. (104). In that context, Zhao et al. has demonstrated that enzymes in the glycolysis cascade undergo sequential chemotaxis to form micron-sized aggregates upon introduction of the substrate for the first enzyme (29). This study highlights the relevance of enzyme chemotaxis in biology. Similar metabolon formation via chemotaxis was also reported by the Minteer group employing Kreb's cycle enzymes, malate dehydrogenase, and citrate synthase (30). Several other studies also provide evidence for the critical role of enzyme cascade reactions in biological self-assembly and transport phenomena (34, 92, 105, 106).

5.2. Applications of Enzyme Motility in In Vivo and In Vitro Studies

The construction of novel hybrid motors by attaching enzymes as functional engines on synthetic particles and propelling them via catalysis looks promising for therapeutics and toxin removal, and for monitoring the environment (107–109). Such nanomotors were found to exhibit enhanced performance as drug delivery vehicles and accelerated drug release kinetics upon catalysis compared to the passive counterparts (26). Pioneering work on these biohybrid systems for in vivo and in vitro applications has come from the Sanchez and Wilson groups (107–115). A recent series of articles have highlighted surface functionalization of silica mesoporous particles with urease in developing motors that shows high efficiency for targeting cancer cells with drugs like doxorubicin (**Figure *6a*,*b***) or antibodies like anti-FGFR3 (107, 108). The motors show enhanced cell penetration when substrate is either externally added or inherently produced in the medium and the delivery at target sites is stimulated by environmental conditions such as pH changes. In another study, the combination of a DNA nanoswitch and urease-functionalized silica micromotors has been designed to sense the pH of the surrounding medium. As the urease nanomotor undergoes enhanced diffusion in urea solution, the latter is decomposed to ammonia, which increases the pH of the solution. The attached DNA nanoswitch changes conformation due to pH change, which was monitored by Förster resonance energy transfer (109). A key to enhanced actuation of synthetic particles lies in the number of enzymes and their spatial distribution on their surface. Patiño et al. could precisely quantify the number of enzymes attached to a particle surface using high-resolution STORM (46); other groups have showed that sodium dodecyl sulphate–polyacrylamide gel electrophoresis experiments are also a convenient tool to estimate the number of enzymes attached per colloidal particle (40, 71, 115, 117). The bowl-shaped polymersome stomatocytes developed by Wilson and coworkers (75) were shown to host compartmentalized

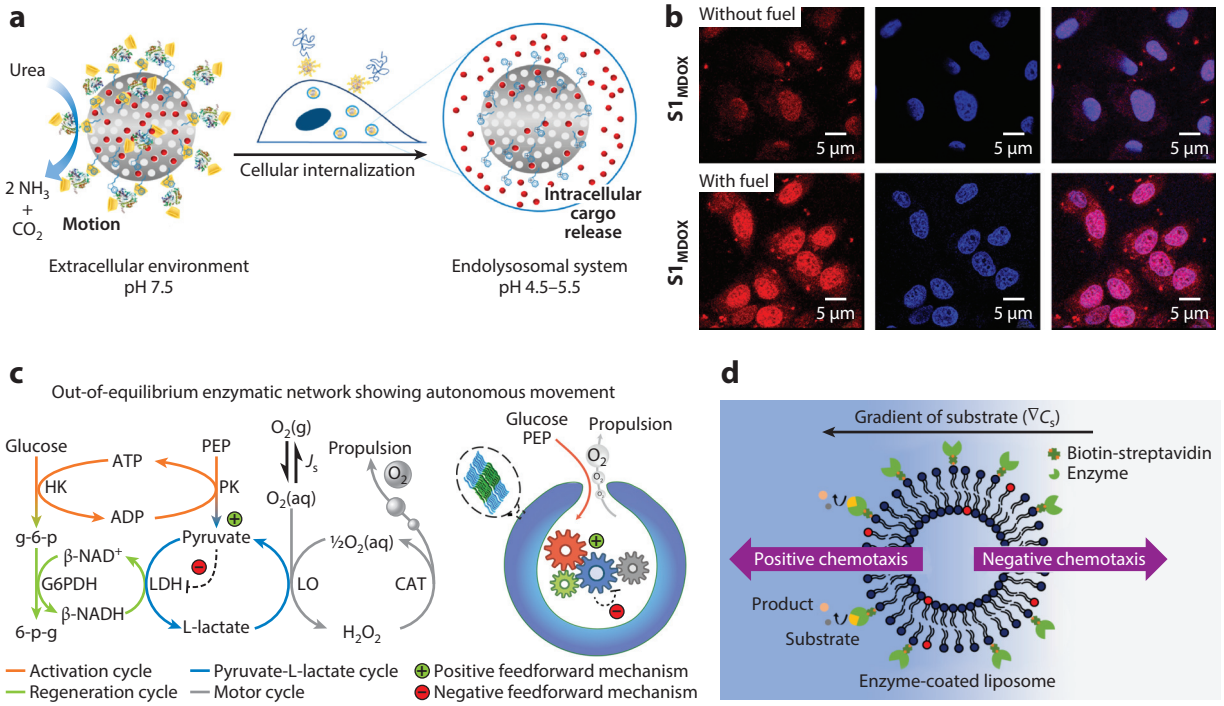

Figure 6

(*a*) Schematic representation of urease-functionalized biocatalytic nanomotors, which exhibit enhanced diffusion due to the enzymatic conversion of urea and release their cargo at acidic pH inside the cell. (*b*) Confocal microscopy images of HeLa cells treated with $S1_{MDOX}$ (urease nanomotors loaded with doxorubicin) in the absence and presence of 50 mM of urea. The fluorescence channels from left to right represent dox (*red*), DNA-marker Hoechst 3342 (*blue*), and merged image (*purple* and *magenta*). (*c*) Schematic representation of the stomatocytes incorporating the enzyme cascade and the metabolic pathway leading to out-of-equilibrium autonomous movement. (*d*) Schematic illustration of liposomes decorated with surface enzymes that show directional migration toward or away from the substrate depending on specific chemical cues. Panels *a* and *b* adapted with permission from Reference 107; copyright 2019 American Chemical Society. Panel *c* adapted with permission from Reference 116; copyright 2016 American Chemical Society. Panel *d* adapted with permission from Reference 71; copyright 2019 Springer Nature. Abbreviations: ADP, adenosine diphosphate; ATP, adenosine triphosphate; Cat, catalase; MDOX, doxorubicin loaded nanomotor; G6PDH, glucose-6-phosphate dehydrogenase; g-6-p, glucose-6-phosphate; 6-p-g, 6-phosphogluconolactone; HK, hexokinase; LO, L-lactate oxidase; LDH, L-lactate dehydrogenase; PK, pyruvate kinase; PEP, phosphoenolpyruvate.

metabolic activity through an enzyme cascade network and produce sustained movement in the presence of the initial substrate (**Figure 6*c***) (116). Furthermore, the phoretic self-propulsion of these stomatocytes has been exploited for various biomedical applications (112, 113). When decorated with different biological entities, they were claimed to be more biocompatible and stable, in comparison with Janus biohybrids (118). Sun et al. fabricated ultrasmall 150-nm stomatocytes that amplified their ability to penetrate pulmonary artery endothelial cells and HeLa cells (115). Similarly, polymersomes carrying individual or a combination of enzymes have been shown to move directionally toward higher-concentration regions in response to a gradient of the substrate. By functionalizing these polymersomes with a specific combination of biomolecules, the nanoswimmers exhibited enhanced transport across the blood–brain barrier (76). Despite active polymersomes and Janus particles being efficiently tuned as model cell mimics, liposomes may hold the edge due to their close resemblance to the cell membranes (119). In this context, Somasundar et al. showed that liposomes are excellent candidates as biocompatible vehicles for drug or cargo

delivery (71). The liposomes that they reported were rendered active by enzyme attachment on the surface or by reconstitution inside the membrane. They display excellent control over directionality in response to chemical cues, showing reconfigurable motion depending on their surface architecture (**Figure 6*d***). Furthermore, the observation of enhanced diffusion of these liposomes during catalysis makes them key models in the elucidation of the fundamental mechanisms governing active membrane dynamics (40). The enzyme-powered pumps were also successfully demonstrated for possible applications in drug delivery and sensing of analytes by harnessing the chemical energy from catalysis (25, 94).

6. FUTURE DIRECTIONS

Although enzyme self-propulsion has been established, several key questions remain. The determination of the precise mechanism governing reaction-dependent motility is important for its applications in biomedical fields, along with accurate control over the motion directionality and the ability to move against fluid flow. Furthermore, most diffusion studies on enzymes have been performed in aqueous media, in contrast to non-Newtonian viscous biological fluids like blood, which have multiple constituents such as plasma, platelets, red and white blood cells, and dissolved ions (28). Their effects on active enzyme motility need to be studied. Although recent calculations suggest that the mechanical forces arising from enzymatic turnover are sufficient for self-propulsion (1, 12, 23), it is unclear whether these forces can drive enzymes or enzyme-anchored species against fluid flow and generate biologically relevant events. These studies are particularly important in the application of adaptive biohybrids that can interact and respond to their environment (120). For example, a biohybrid adaptive machine fabricated by tethering muscle cells to synthetic materials can respond to an electrical signal triggered by contractile forces of myosin motors (121). From a technological perspective, whether catalytic processes can drive lab-on-a-chip devices provides the impetus behind the study of enzyme-based synthetic motors and pumps (6). Although many self-powered nano- and/or micromotors have been reported, their biocompatibility and their viability in the presence of harsh external conditions remain a concern (113). The surface functionalization of nano- and/or micromotors with enzymes would ensure necessary biocompatibility, and catalytic propulsion would assist in faster cell uptake. In contrast to attachment of enzymes of a single type, introduction of orthogonality via multiple enzymes might facilitate greater control of directed motion and additional functionalities (76). Future studies should focus on substrates that are biocompatible and preferably available in the body as demonstrated in a recent work on antibody-modified nanomotors (108). Response mechanisms triggered by pH, thermal, or chemical gradients need to be examined more closely for enzyme-based molecular machines with applications in efficient drug delivery, cell targeting, and other theranostic applications (71, 109, 115, 120). Intelligent molecular machines undergoing self-organization via signaling can be developed based on chemotactic migration in enzyme cascades through positive feedback (29). Similarly, developing biomachines acting through a network of negative feedbacks is equally important in understanding dynamic principles underlying life processes. Due to flexibility and cell-like rheological properties, soft nano- and/or microhybrids like enzyme-powered liposomes or cell-powered microrobots have garnered interest as novel cell mimics and cargo delivery vehicles (121).

7. CONCLUSION

Enzymes have been shown to display active motion when catalyzing substrates into products and harnessing the resultant chemical energy into mechanical force. The cell contains proteins such as myosins, kinesins, and dyneins that perform motor activity for cargo transport and are responsible for stochastic motion of the cytoplasm by drawing energy from ATP hydrolysis. Over the past

decade, researchers have been particularly focused on the behavior of non-ATP-driven enzymes, particularly those that are freely dispersed in solution. These enzymes have been shown to exhibit enhanced diffusive motion under out-of-equilibrium conditions. Furthermore, they can move directionally up a gradient of substrate, mimicking the behavior of cellular chemotaxis in vitro. In most cases, self-propulsion shows strong substrate concentration dependence and Michaelis–Menten-type kinetics. Although several mechanisms like phoresis, conformational fluctuations, or local asymmetry have been proposed, the precise propulsive mechanism remains unclear. Utilizing force generation through catalysis, chemically-powered catalytic motors and pumps have been constructed by attaching enzymes as functional engines on inorganic particles or a solid support for potential actuation in therapeutic and toxin-removal applications, and for monitoring the environment. Further studies have shown that enzymes can communicate through chemical signaling in cascade reactions, giving rise to metabolon formation or construction of adaptive and internally regulated life-like systems. Model cell mimics have been fabricated using enzyme-attached liposomes, polymersomes, and Janus particles, which, besides being biocompatible, serve as potential candidates in drug delivery, sensing, and different cellular activities. Despite these successes, exploring enzyme motility in vivo is in its infancy due to the stochastic nature of the system and limitations of experimental and theoretical techniques in characterizing nonequilibrium systems.

SUMMARY POINTS

1. Motion in biological systems stems from enzyme motility at low Reynolds numbers that result from the conversion of chemical energy into mechanical work. The classical picture dates back to the discovery of motor proteins that catalyse ATP hydrolysis to drive cargo on a predefined path within the cell.
2. More recently, freely dispersed non-ATP-dependent enzymes in solution have been shown to display enhanced motility under out-of-equilibrium conditions. The observed self-propulsive behavior of enzymes was found to show substrate concentration dependence following Michaelis–Menten kinetics.
3. In the presence of a substrate gradient, active enzyme molecules and enzyme-attached particles generally move up the gradient; these are the first examples of chemotaxis outside living systems.
4. Enzymes participating in catalytic cascades undergo sequential chemotaxis to assemble into metabolons.
5. When attached to a solid surface, active enzymes transfer their mechanical force to the surrounding fluid, resulting in convective fluid pumping and particle transport.
6. Active enzymes provide sufficient force for the stochastic motion of the cytoplasm, the organization of metabolons and signaling complexes, and the convective transport of fluid in cells.
7. Recent discoveries have opened a new area of mechanobiology: intrinsic force generation by enzymes and their role in biochemical regulation of cell function.

DISCLOSURE STATEMENT

The authors are not aware of any affiliations, memberships, funding, or financial holdings that might be perceived as affecting the objectivity of this review.

ACKNOWLEDGMENT

Our work was supported by the National Science Foundation (DMR-1420620 and CHE-1740630).

LITERATURE CITED

1. Sengupta S, Dey KK, Muddana HS, Tabouillot T, Ibele ME, et al. 2013. *J. Am. Chem. Soc.* 135:1406–14
2. Dey KK, Zhao X, Tansi BM, Méndez-Ortiz WJ, Córdova-Figueroa UM, et al. 2015. *Nano Lett.* 15:8311–15
3. Ma X, Jannasch A, Albrecht UR, Hahn K, Miguel-López A, et al. 2015. *Nano Lett.* 15:7043–50
4. Ma X, Hortelão AC, Miguel-López A, Sánchez S. 2016. *J. Am. Chem. Soc.* 138:13782–85
5. Ma X, Hortelão AC, Patiño T, Sánchez S. 2016. *ACS Nano* 10:9111–22
6. Zhao X, Gentile K, Mohajerani F, Sen A. 2018. *Acc. Chem. Res.* 51:2373–81
7. Ramaswamy S. 2010. *Annu. Rev. Condens. Matter Phys.* 1:323–45
8. Romanczuk P, Bär M, Ebeling W, Lindner B, Schimansky-Geier L. 2012. *Eur. Phys. J. Spec. Top.* 202:1–162
9. Marchetti MC, Joanny JF, Ramaswamy S, Liverpool TB, Prost J, et al. 2013. *Rev. Mod. Phys.* 85:1143–89
10. Jülicher F, Grill SW, Salbreux G. 2018. *Rep. Prog. Phys.* 81:076601
11. Purcell EM. 1977. *Am. J. Phys.* 45:3
12. Butler PJ, Dey KK, Sen A. 2015. *Cell Mol. Bioeng.* 8:106–18
13. Berg HC. 1993. *Random Walks in Biology*. Princeton, NJ: Princeton Univ. Press
14. Hoyt MA, Hyman AA, Bähler M. 1997. *PNAS* 94:12747–48
15. Vale RD, Milligan RA. 2000. *Science* 288:88–95
16. Roberts AJ, Kon T, Knight PJ, Sutoh K, Burgess SA. 2013. *Nat. Rev. Mol. Cell Biol.* 14:713–26
17. Goel A, Vogel V. 2008. *Nat. Nanotechnol.* 3:465–75
18. Alberts B, Johnson A, Lewis J, Raff M, Roberts K, et al. 2002. *Molecular Biology of the Cell*. New York: Garland Sci.
19. Spudich JA, Rice SE, Rock RS, Purcell TJ, Warrick HM. 2011. *Cold Spring Harb. Protoc.* 2011:1305–18
20. Mikhailov AS, Kapral R. 2015. *PNAS* 112:E3639–44
21. Agudo-Canalejo J, Adeleke-Larodo T, Illien P, Golestanian R. 2018. *Acc. Chem. Res.* 51:2365–72
22. Golestanian R, Liverpool TB, Ajdari A. 2005. *Phys. Rev. Lett.* 94:220801
23. Muddana HS, Sengupta S, Mallouk TE, Sen A, Butler PJ. 2010. *J. Am. Chem. Soc.* 132:2110–11
24. Xu M, Ross JL, Valdez L, Sen A. 2019. *Phys. Rev. Lett.* 123:128101
25. Sengupta S, Patra D, Ortiz-Rivera I, Agrawal A, Shklyaev S, et al. 2014. *Nat. Chem.* 6:415–22
26. Hortelão AC, Patiño T, Perez-Jiménez A, Blanco A, Sánchez S. 2018. *Adv. Funct. Mater.* 28:1705086
27. Walker D, Käsdorf BT, Jeong HH, Lieleg O, Fischer P. 2015. *Sci. Adv.* 1:e1500501
28. Dey KK, Sen A. 2017. *J. Am. Chem. Soc.* 139:7666–76
29. Zhao X, Palacci H, Yadav V, Spiering MM, Gilson MK, et al. 2018. *Nat. Chem.* 10:311–17
30. Wu F, Pelster LN, Minteer SD. 2015. *Chem. Comm.* 51:1244–47
31. Sengupta S, Spiering MM, Dey KK, Duan W, Patra D, et al. 2014. *ACS Nano* 8:2410–18
32. Illien P, Zhao X, Dey KK, Butler PJ, Sen A, Golestanian R. 2017. *Nano Lett.* 17:4415–20
33. Zhao X, Dey KK, Jeganathan S, Butler PJ, Córdova-Figueroa UM, Sen A. 2017. *Nano Lett.* 17:4807–12
34. Sun L, Gao Y, Xu Y, Chao J, Liu H, et al. 2017. *J. Am. Chem. Soc.* 139:17525–32
35. Börsch M, Turina P, Eggeling C, Fries JR, Seidel CA, et al. 1998. *FEBS Lett.* 437:251–54
36. Günther JP, Börsch M, Fischer P. 2018. *Acc. Chem. Res.* 51:1911–20
37. Bai X, Wolynes PG. 2015. *J. Chem. Phys.* 143:165101
38. Paliwal S, Wales M, Good T, Grimsley J, Wild J, Simonian A. 2007. *Anal. Chim. Acta.* 596:9–15
39. Zhang Y, Hess H. 2019. *ACS Cent. Sci.* 5:939–48
40. Ghosh S, Mohajerani F, Son S, Velegol D, Butler PJ, Sen A. 2019. *Nano Lett.* 19:6019–26
41. Arqué X, Romero-Rivera A, Feixas F, Patiño T, Osuna S, Sánchez S. 2019. *Nat. Comm.* 10:2826
42. Incicco JJ, Gebhard LG, González-Lebrero RM, Gamarnik AV, Kaufman SB. 2013. *PLOS ONE* 8:e58508

43. Jee AY, Dutta S, Cho YK, Tlusty T, Granick S. 2018. *PNAS* 115:14–18
44. Leckie J, Hope A, Hughes M, Debnath S, Fleming S, et al. 2014. *ACS Nano* 8:9580–89
45. Jiang L, Santiago I, Foord J. 2017. *Chem. Comm.* 53:8332–35
46. Patiño T, Feiner-Gracia N, Arqué X, Miguel-López A, Jannasch A, et al. 2018. *J. Am. Chem. Soc.* 140:7896–903
47. Feng M, Gilson MK. 2020. *Annu. Rev. Biophys.* 49:87–105
48. Yu H, Jo K, Kounovsky KL, de Pablo JJ, Schwartz DC. 2009. *J. Am. Chem. Soc.* 131:5722–23
49. Golestanian R. 2009. *Phys. Rev. Lett.* 102:188305
50. Riedel C, Gabizon R, Wilson CA, Hamadani K, Tsekouras K, et al. 2015. *Nature* 517:227–30
51. Leitner DM. 2008. *Annu. Rev. Phys. Chem.* 59:233–59
52. Golestanian R. 2015. *Phys. Rev. Lett.* 115:108102
53. Zhang Y, Armstrong MJ, Bassir Kazeruni NM, Hess H. 2018. *Nano Lett.* 18:8025–29
54. Günther JP, Majer G, Fischer P. 2019. *J. Chem. Phys.* 150:124201
55. Dennison M, Kapral R, Stark H. 2017. *Soft Matter* 13:3741–49
56. Sakaue T, Kapral R, Mikhailov A. 2010. *Eur. Phys. J. B* 75:381–87
57. Jee AY, Chen K, Tlusty T, Zhao J, Granick S. 2019. *J. Am. Chem. Soc.* 141:20062–68
58. Yin H, Wang MD, Svoboda K, Landick R, Block SM, Gelles J. 1995. *Science* 270:1653–57
59. Mehta AD, Rief M, Spudich JA, Smith DA, Simmons RM. 1999. *Science* 283:1689–95
60. Mahadevan L, Matsudaira P. 2000. *Science* 288:95–100
61. Colberg PH, Kapral R. 2014. *Europhys. Lett.* 106:30004
62. Golestanian R. 2010. *Phys. Rev. Lett.* 105:018103
63. Feng M, Gilson MK. 2019. *Biophys. J.* 116:1898–906
64. Lauga E. 2011. *Phys Rev. Lett.* 106:178101
65. Kondrat S, Popescu MN. 2019. *Phys. Chem. Chem. Phys.* 21:18811–15
66. Jee AY, Cho YK, Granick S, Tlusty T. 2018. *PNAS* 115:E10812–21
67. Agudo-Canalejo J, Illien P, Golestanian R. 2018. *Nano Lett.* 18:2711–17
68. Weistuch C, Pressé S. 2018. *J. Phys. Chem. B* 122:5286–90
69. Xu C, Hu S, Chen X. 2016. *Mater. Today* 19:516–32
70. Wang W, Duan W, Ahmed S, Sen A, Mallouk TE. 2015. *Acc. Chem. Res.* 48:1938–46
71. Somasundar A, Ghosh S, Mohajerani F, Massenburg LN, Yang T, et al. 2019. *Nat. Nanotechnol.* 14:1129–34
72. Mohajerani F, Zhao X, Somasundar A, Velegol D, Sen A. 2018. *Biochemistry* 57:6256–63
73. Wilson DA, Nolte RJ, van Hest JC. 2012. *Nat. Chem.* 4:268–74
74. Peng F, Tu Y, van Hest JC, Wilson DA. 2015. *Angew. Chem. Int. Ed.* 54:11662–65
75. Abdelmohsen LK, Nijemeisland M, Pawar GM, Janssen GJ, Nolte RJ, et al. 2016. *ACS Nano* 10:2652–60
76. Joseph A, Contini C, Cecchin D, Nyberg S, Ruiz-Perez L, et al. 2017. *Sci. Adv.* 3:e1700362
77. Anderson JL. 1983. *Phys. Fluids* 26:2871
78. Nardi J, Bruinsma R, Sackmann E. 1999. *Phys. Rev. Lett.* 82:5168–71
79. Kodama A, Sakuma Y, Imai M, Kawakatsu T, Puff N, Angelova MI. 2017. *Langmuir* 33:10698–706
80. Gupta S, Sreeja KK, Thakur S. 2015. *Phys. Rev. E Stat. Nonlin. Soft Matter Phys.* 92:042703
81. Küchler A, Yoshimoto M, Luginbühl S, Mavelli F, Walde P. 2016. *Nat. Nanotechnol.* 11:409–20
82. Qiao Y, Li M, Booth R, Mann S. 2017. *Nat. Chem.* 9:110–19
83. Pavan Kumar BVVS, Patil AJ, Mann S. 2018. *Nat. Chem.* 10:1154–63
84. Jang WS, Kim HJ, Gao C, Lee D, Hammer DA. 2018. *Small* 14:e1801715
85. Zhang Y, Cremer PS. 2006. *Curr. Opin. Chem. Biol.* 10:658–63
86. Dey KK, Das S, Poyton MF, Sengupta S, Butler PJ, et al. 2014. *ACS Nano* 8:11941–49
87. Ilacas GC, Basa A, Sen A, Gomez FA. 2018. *Anal. Sci.* 34:115–19
88. Saha S, Golestanian R, Ramaswamy S. 2014. *Phys. Rev. E* 89:062316
89. Schurr JM, Fujimoto BS, Huynh L, Chiu DT. 2013. *J. Phys. Chem. B* 117:7626–52
90. Sitt A, Hess H. 2015. *Nano Lett.* 15:3341–50
91. Zhang C, Sitt A, Koo HJ, Waynant KV, Hess H, et al. 2015. *J. Am. Chem. Soc.* 137:5066–73
92. Maiti S, Shklyaev OE, Balazs AC, Sen A. 2019. *Langmuir* 35:3724–32

93. Alarcón-Correa M, Günther JP, Troll J, Kadiri VM, Bill J, et al. 2019. *ACS Nano* 13:5810–15
94. Ortiz-Rivera I, Courtney TM, Sen A. 2016. *Adv. Funct. Mater.* 26:2135–42
95. Ortiz-Rivera I, Shum H, Agrawal A, Sen A, Balazs AC. 2016. *PNAS* 113:2585–90
96. Valdez L, Shum H, Ortiz-Rivera I, Balazs AC, Sen A. 2017. *Soft Matter* 13:2800–7
97. Das S, Shklyaev OE, Altemose A, Shum H, Ortiz-Rivera I, et al. 2017. *Nat. Commun.* 8:14384
98. Laskar A, Shklyaev OE, Balazs AC. 2019. *PNAS* 116:9257–62
99. Vale RD. 2003. *Cell* 112:467–80
100. Freedman RB. 1981. *New Compr. Biochem.* 1:161–214
101. Dufrêne YF, Evans E, Engel A, Helenius J, Gaub HE, Müller DJ. 2011. *Nat. Methods* 8:123–27
102. Yamada S, Wirtz D, Kuo SC. 2000. *Biophys. J.* 78:1736–47
103. Guo M, Ehrlicher AJ, Jensen MH, Renz M, Moore JR, et al. 2014. *Cell* 158:822–32
104. Zhao X, Sen A. 2019. *Methods Enzymol.* 617:45–62
105. Seger R, Krebs EG. 1995. *FASEB J.* 9:726–35
106. Zhang Y, Hess H. 2017. *ACS Catal.* 7:6018–27
107. Llopis-Lorente A, García-Fernández A, Murillo-Cremaes N, Hortelão AC, Patiño T, et al. 2019. *ACS Nano* 13:12171–83
108. Hortelão AC, Carrascosa R, Murillo-Cremaes N, Patiño T, Sánchez S. 2019. *ACS Nano* 13:429–39
109. Patiño T, Porchetta A, Jannasch A, Lladó A, Stumpp T, et al. 2019. *Nano Lett.* 19:3440–47
110. Xu D, Wang Y, Liang C, You Y, Sánchez S, Ma X. 2020. *Small* 16(27):e1902464
111. Wang L, Song S, van Hest J, Abdelmohsen LKEA, Huang X, Sánchez S. 2020. *Small* 16(27):e1907680
112. Ou J, Liu K, Jiang J, Wilson DA, Liu L, et al. 2020. *Small* 16(27):e1906184
113. Keller S, Toebes BJ, Wilson DA. 2019. *Biomacromolecules* 20:1135–45
114. Tu Y, Peng F, André AA, Men Y, Srinivas M, Wilson DA. 2017. *ACS Nano* 11:1957–63
115. Sun J, Mathesh M, Li W, Wilson DA. 2019. *ACS Nano* 13:10191–200
116. Nijemeisland M, Abdelmohsen LK, Huck WT, Wilson DA, van Hest JC. 2016. *ACS Cent. Sci.* 2:843–49
117. Toebes BJ, Cao F, Wilson DA. 2019. *Nat. Commun.* 10:5308
118. Messager L, Gaitzsch J, Chierico L, Battaglia G. 2014. *Curr. Opin. Pharmacol.* 18:104–11
119. Tu Y, Peng F, Adawy A, Men Y, Abdelmohsen LK, Wilson DA. 2016. *Chem. Rev.* 116:2023–78
120. Peng F, Tu Y, Wilson DA. 2017. *Chem. Soc. Rev.* 46:5289–310
121. Patiño T, Mestre R, Sánchez S. 2016. *Lab Chip* 16:3626–30